

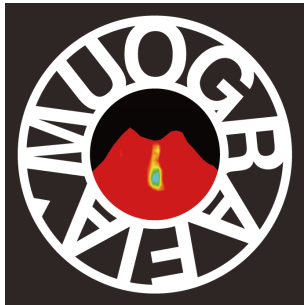
# Muography of the active Sakurajima volcano: recent results and future perspectives of hazard assessment

**László Oláh<sup>1,2</sup>, Hiroyuki K. M. Tanaka<sup>1,2</sup>, Takao Ohminato<sup>2</sup>,  
Gergő Hamar<sup>1,3</sup>, Gábor Nyitrai<sup>1,3</sup>, and Dezső Varga<sup>1,3</sup>**

<sup>1</sup>International Virtual Muography Institute, Global

<sup>2</sup>Earthquake Research Institute, The University of Tokyo, Japan

<sup>3</sup>Wigner RCP, Eötvös Loránd Research Network, Hungary



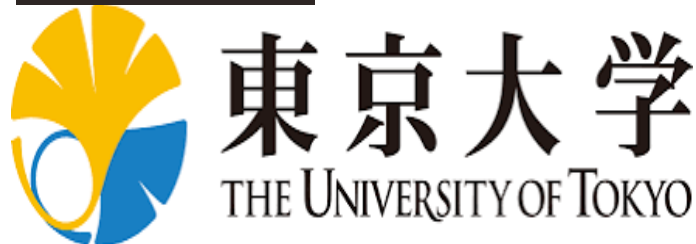
24<sup>th</sup> November 2021



MEXT

MINISTRY OF EDUCATION,  
CULTURE, SPORTS,  
SCIENCE AND TECHNOLOGY-JAPAN

ELKH | Eötvös Loránd  
Research Network



# Outline

**I. Motivation**

**II. Sakurajima Muography Observatory**

**III. Muographic Monitoring of Tephra Deposition and Erosion**

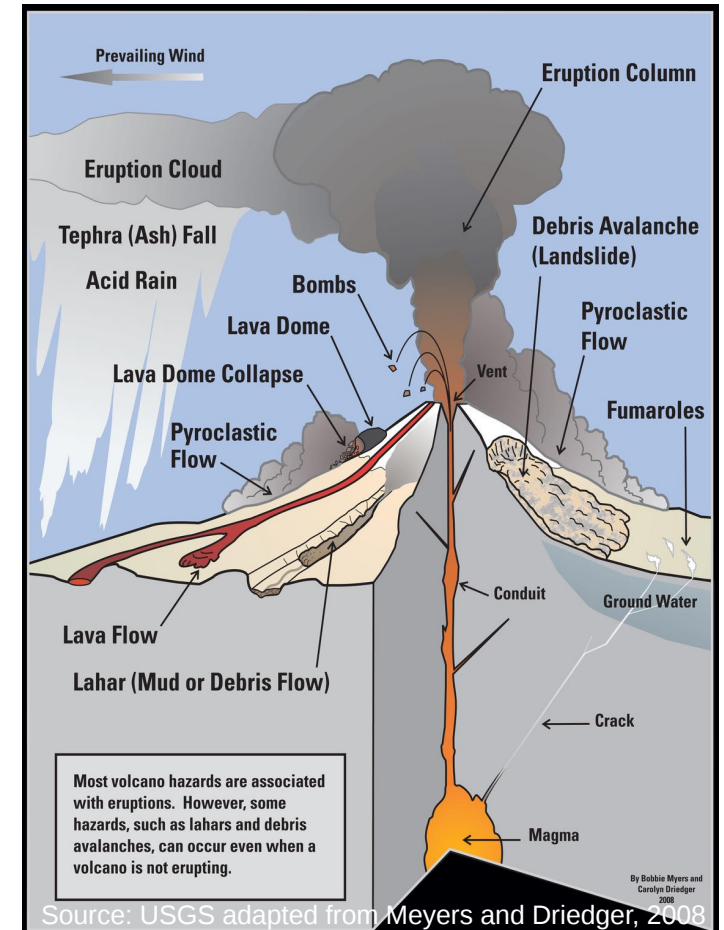
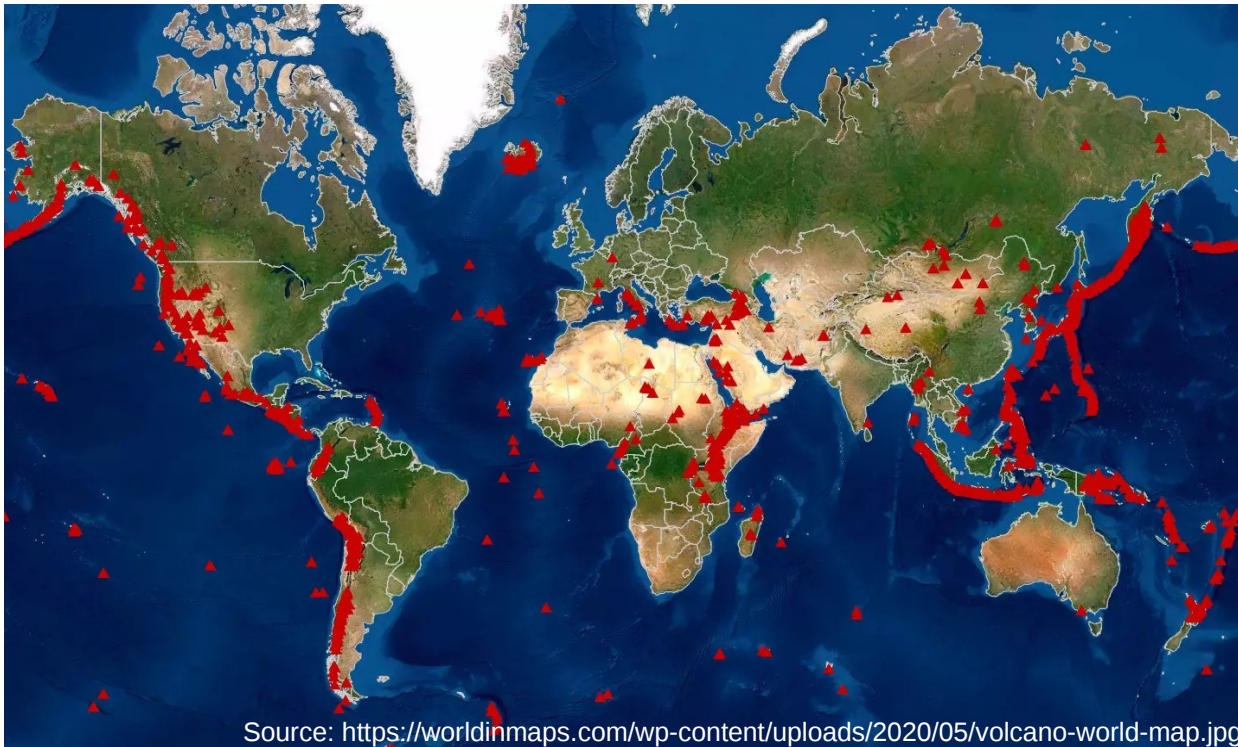
**IV. Muography of Magmatic Plug Formation**

**V. Eruption Forecasting by Machine Learning of Muographic Data**

**VI. Summary**

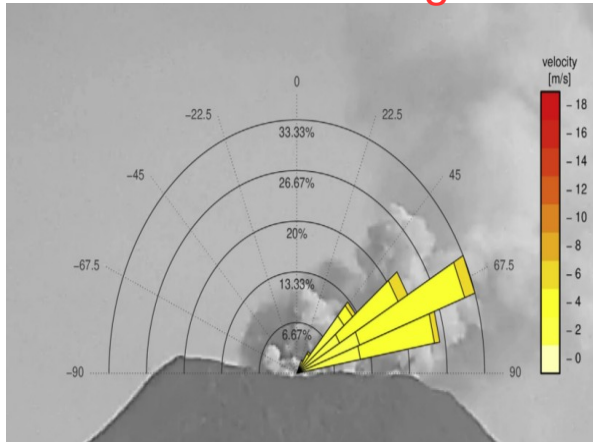
# I. Motivation: Volcanic Hazards

- More than 500 volcanoes confirmed historical eruptions (69 volcanoes erupted in 2021)
- Approx. 10 % of Earth's population live around volcanoes
- Volcanic hazards can cause serious socioeconomic loss:
  - syn-eruptive hazards: bombs, tephra fall, pyroclastic flows, etc
  - post-eruptive hazards: lahars, debris avalanche, etc



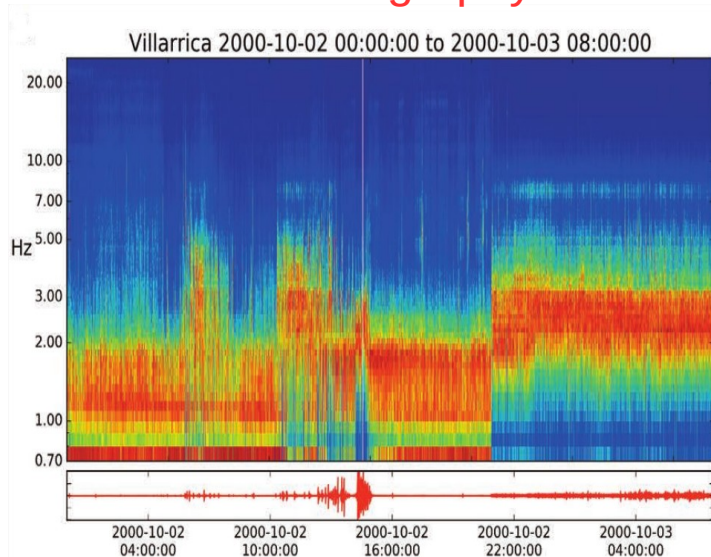
# Volcano Monitoring

## Video recording

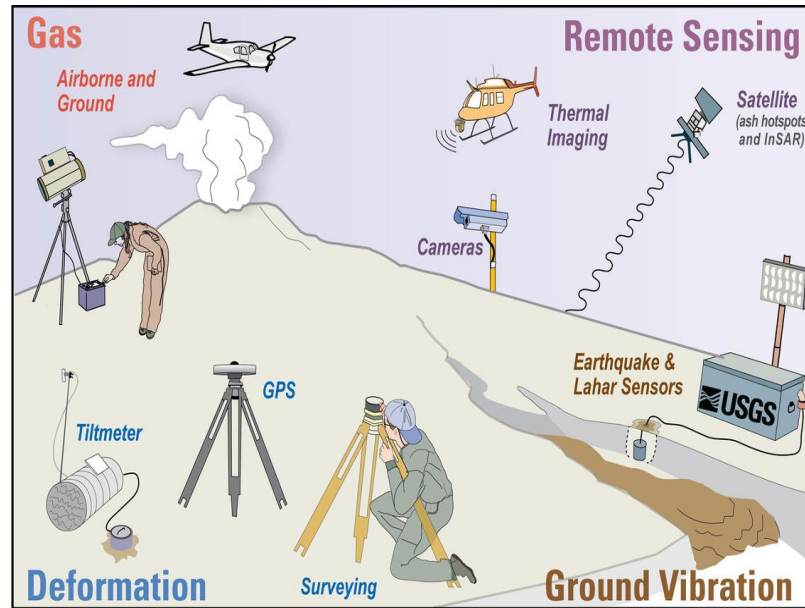


Source: <https://doi.org/10.1016/j.gsf.2020.01.016>

## Seismography

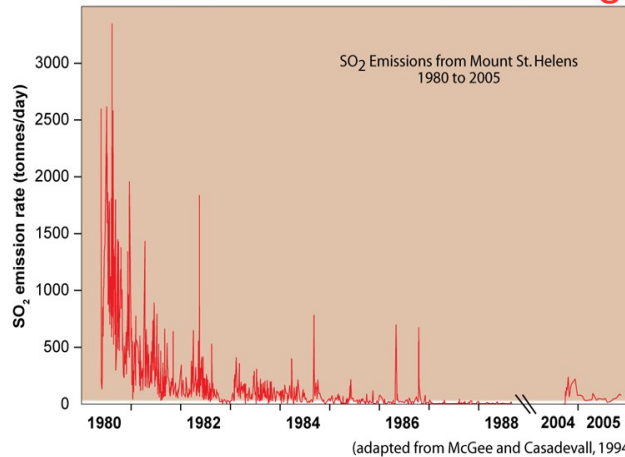


Source: <https://doi.org/10.4401/ag-7655>



Source: USGS from Faust, Lisa

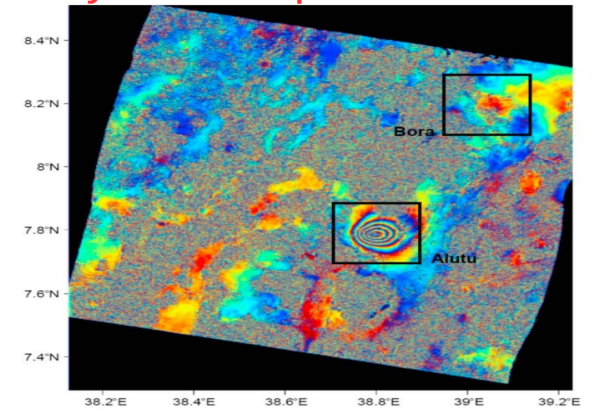
## Gas Emission Monitoring



Source: USGS

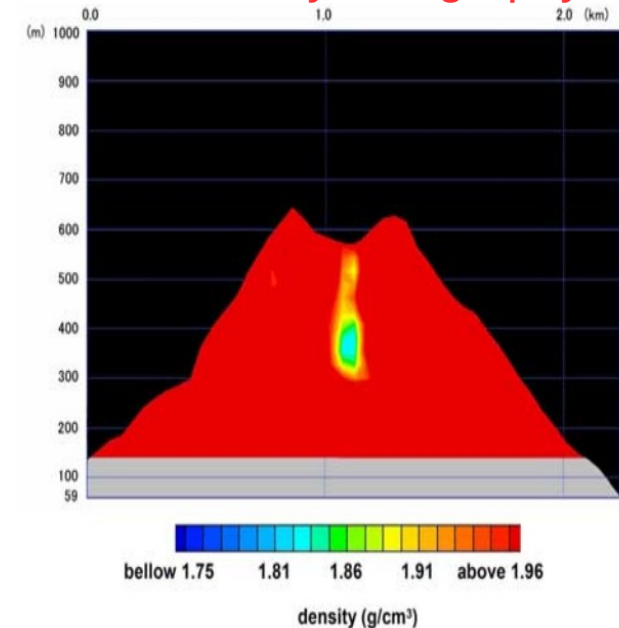
## Oláh Muographers2021

## Synthetic Aperture Radar



Source: <https://doi.org/10.1029/2018JB015911>

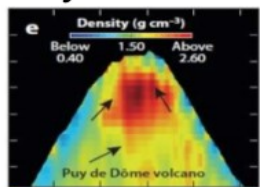
## Cosmic-ray Muography



Source: <https://doi.org/10.1029/2008GL036451>

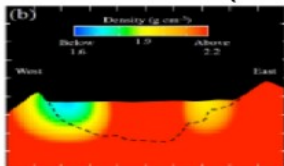
# World-wide Volcano Muography

Puy de Dome (FR)



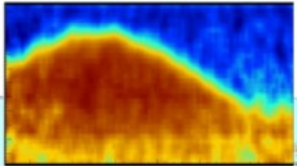
Carloganu et al. 2012

Kirishima (JP)

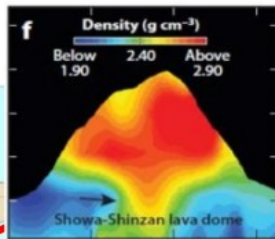


Kusagaya and Tanaka 2015

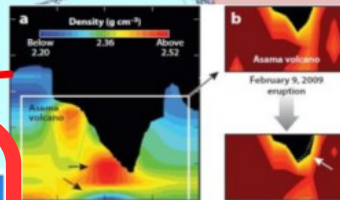
Saracino et al. 2017  
Vesuvio (IT)



Showa-shinzan (JP) Tanaka et al. 2007



Soufrier Hills (UK) underway

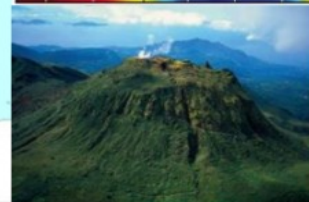
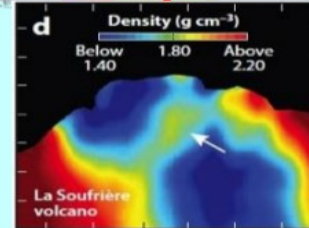
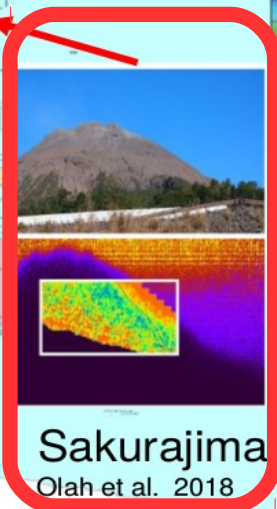


Asama (JP)

Tanaka et al. 2007

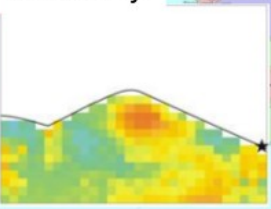
Sakurajima (JP)

Olah et al. 2018

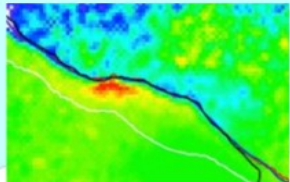


Lesparre et al. 2012 La Soufriere (FI)

Canary Islands (ES) underway

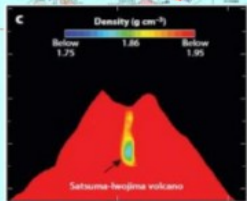


Carbone et al. 2014  
Etna (IT)



Stromboli (IT)

Tioiukov et al. 2017



Satsuma Iwojima (JP)

Tanaka et al. 2008

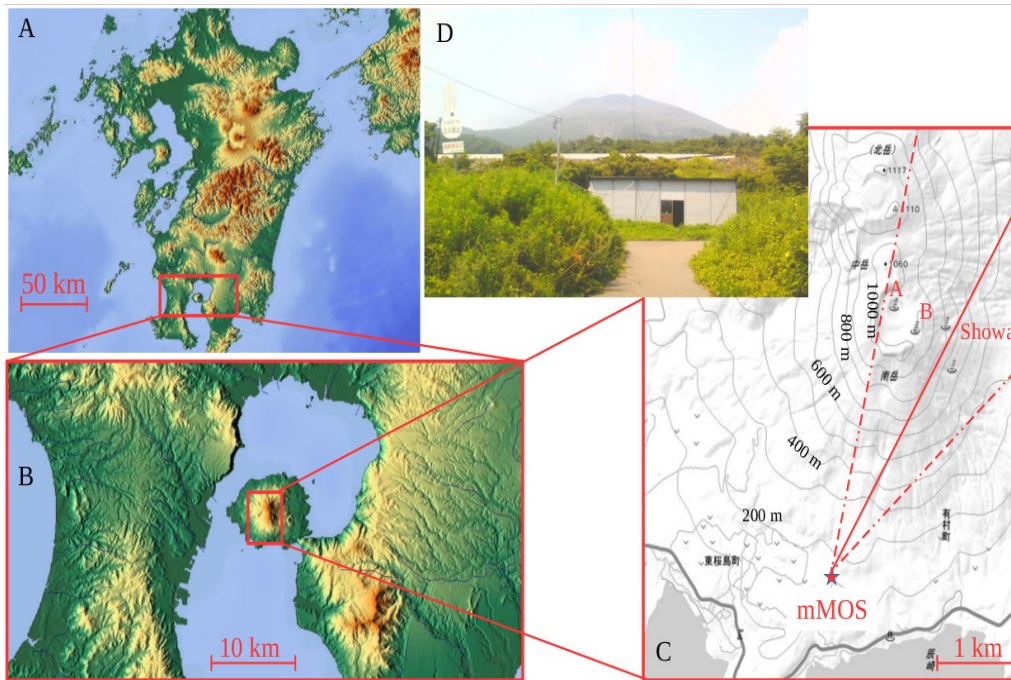
See more in talks by  
Jesus Peña Rodriguez (MuTe),  
Mariaelena D'Errico and Marwa Al Moussawi (MURAVES),  
Raphael Bajou (DIAPHANE).

Oláh Muographers2021

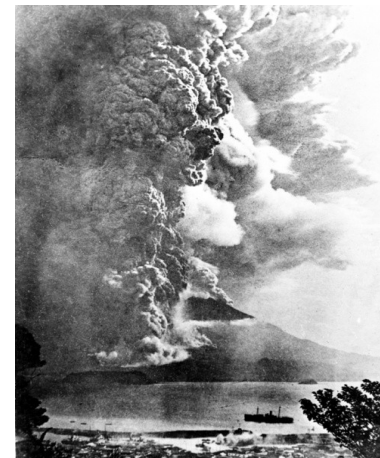
Source: H. K. M. Tanaka

# The Sakurajima Volcano, Kyushu, Japan

- Sakurajima volcano is an active stratovolcano on the "Ring of fire" within the Aira caldera in Kagoshima Bay
- Latest plinian eruption occurred in 1914 → Next plinian eruption is expected in 25 years  
<https://doi.org/10.1038/srep32691>
- Two craters of the southern peak (the connected Vents A and B, as well as Showa crater) erupted consecutively in the recent years → A few hundreds of (explosive) short-term eruptions per year
- Short-term eruptions eject aerosols and gas with a bulk volume of below  $10^7 \text{ m}^3$  to a height of 1000–5000 meter above the crater rims, throwing fragments of volcanic plug and lava bombs usually within approx. 3000 m radius
- **Protection of tourists motivates the forecasting of short-term eruptions of the Sakurajima volcano**



Source: <https://doi.org/10.1038/s41598-018-21423-9>



Source: Wikipedia



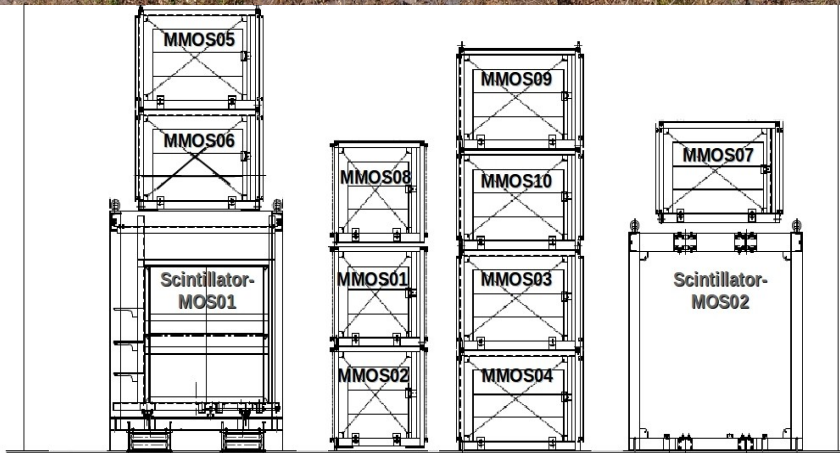
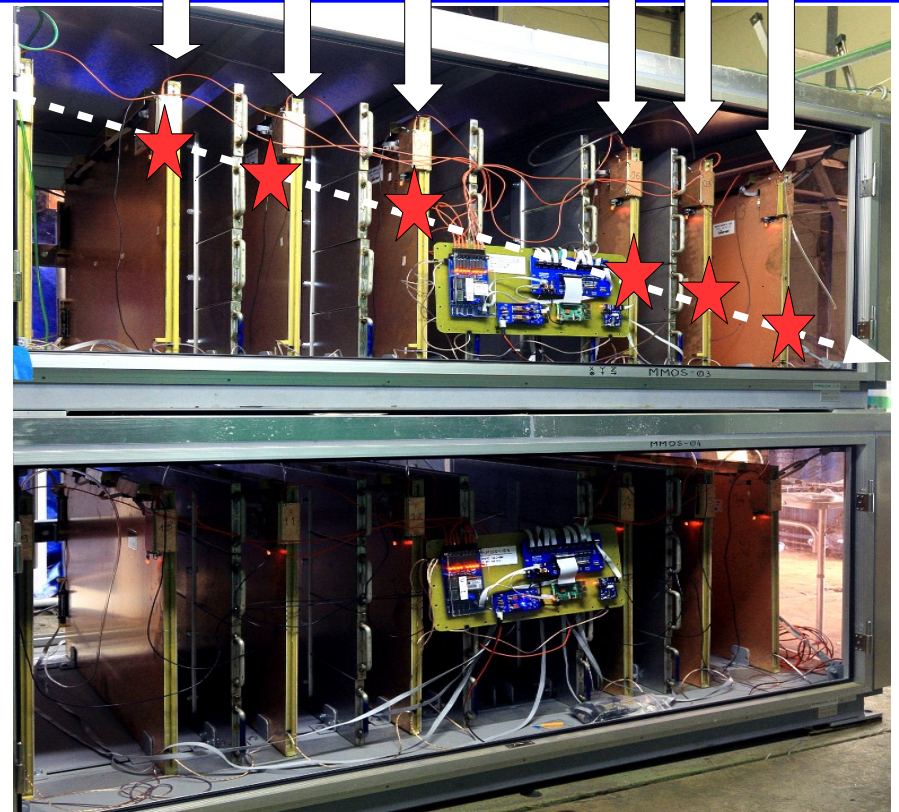
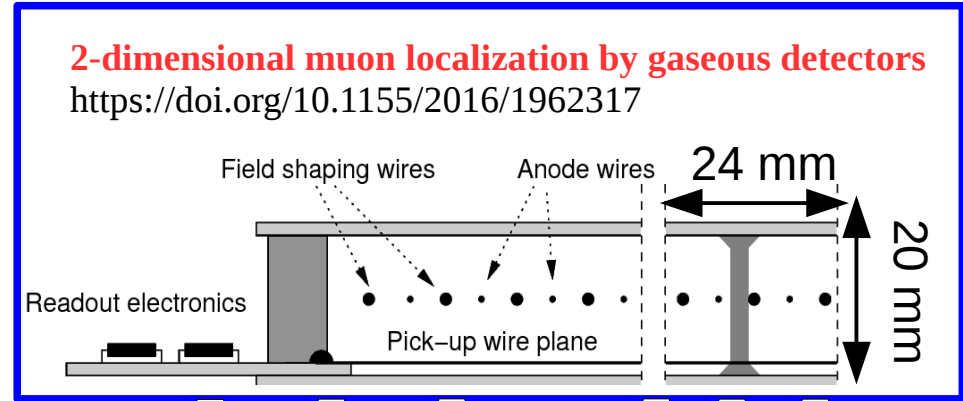
Source: Kimon Berlin, CC BY-SA 2.0

# II. Sakurajima Muography Observatory

# II. Sakurajima Muography Observatory

Multi-Wire Proportional Chamber (MWPC)-based Muography Observation System (MMOS)

See more in the talk by Dezső Varga



**2017: 0.6 m<sup>2</sup>**      **2018: 3.6 m<sup>2</sup>**      **2021: 8.7 m<sup>2</sup>** →

Patent: Muographic Observation Instrument (WO 2017/187308 A1)

Publications:

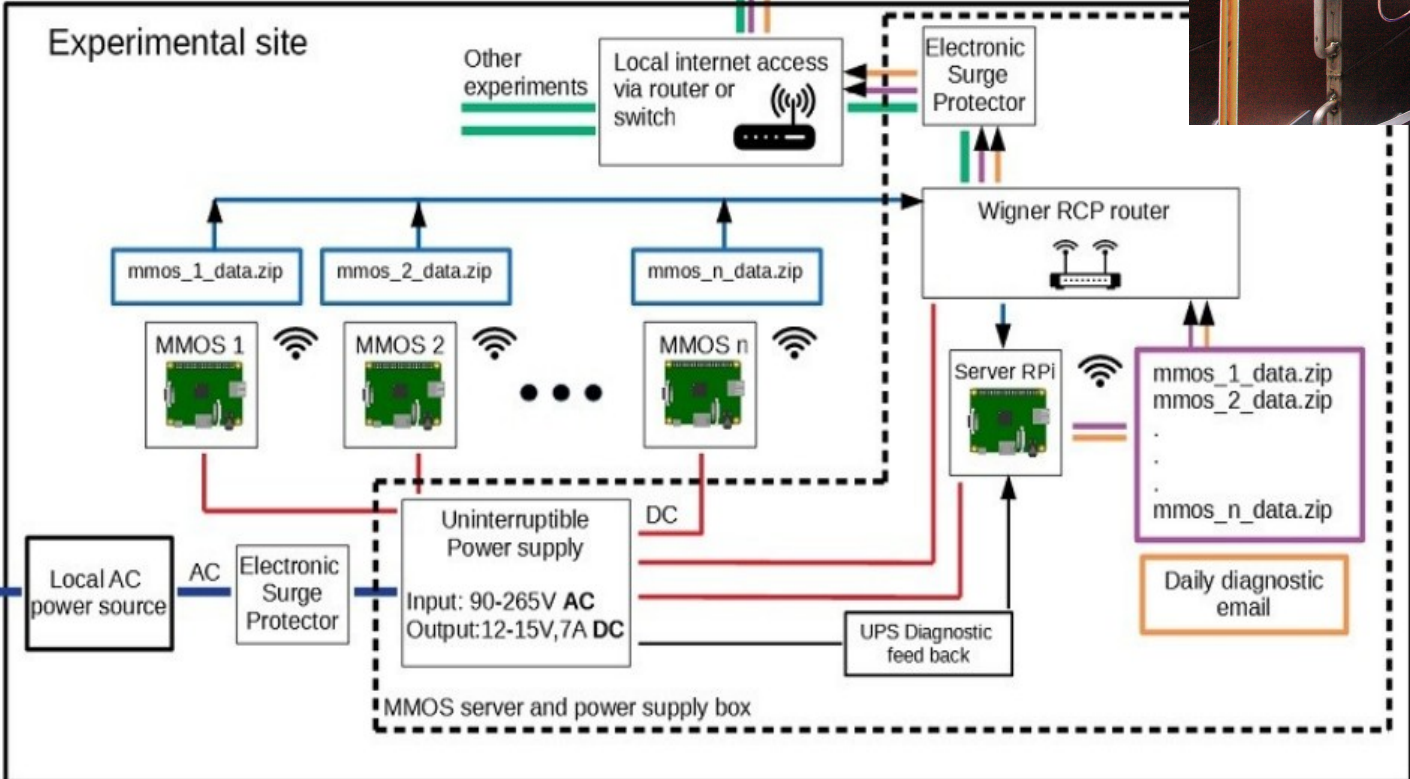
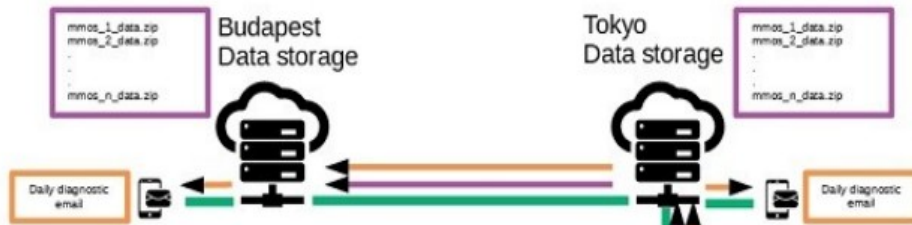
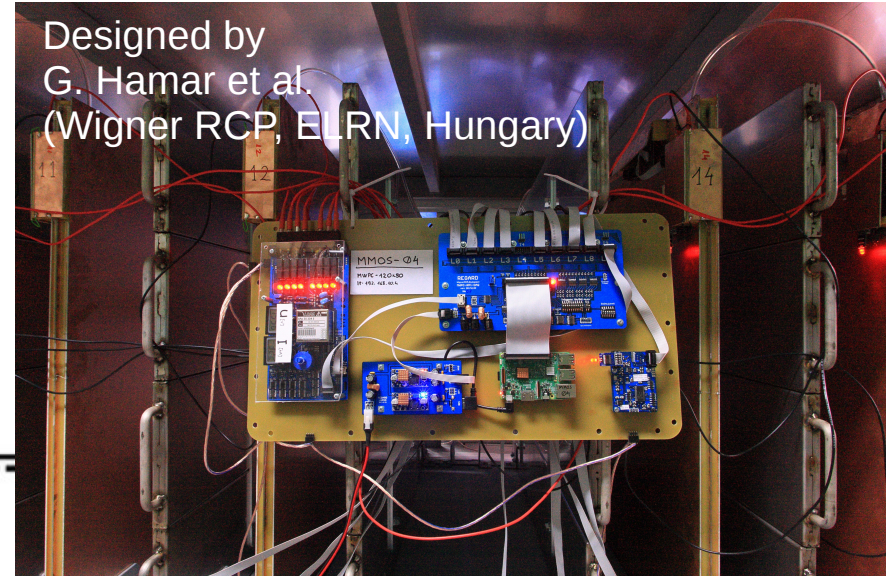
<https://doi.org/10.1038/s41598-018-21423-9>

<https://doi.org/10.1029/2019GL084784>

<https://doi.org/10.1016/j.nima.2019.05.077>

Oláh Muographers2021

# System Plan: Data Acquisition



- Custom-designed electronics
- Power consumption:  
~ 6 W per MMOS
- **Micro-computer controlled**  
→ **real-time DAQ & analysis**
- Data transferred and stored on remote computers

Source: Szabolcs József Balogh (Wigner RCP, ELRN, Hungary)  
See more in Varga et al.  
<https://doi.org/10.1016/j.nima.2019.05.077>

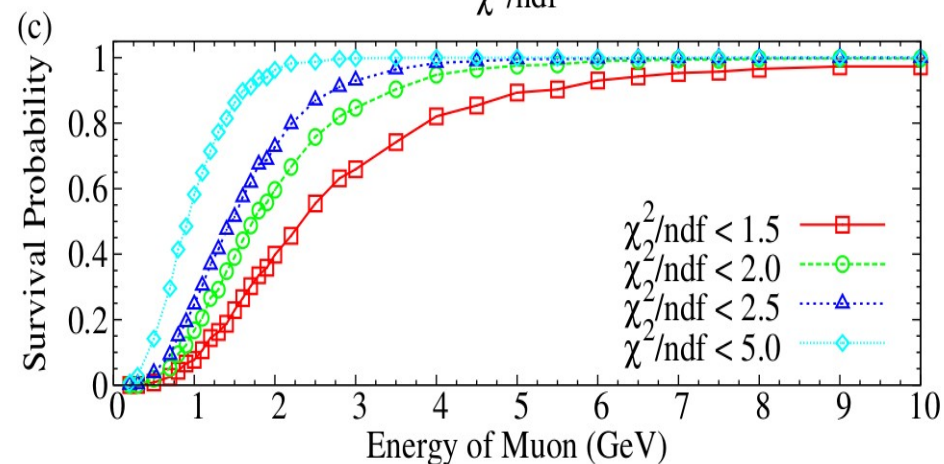
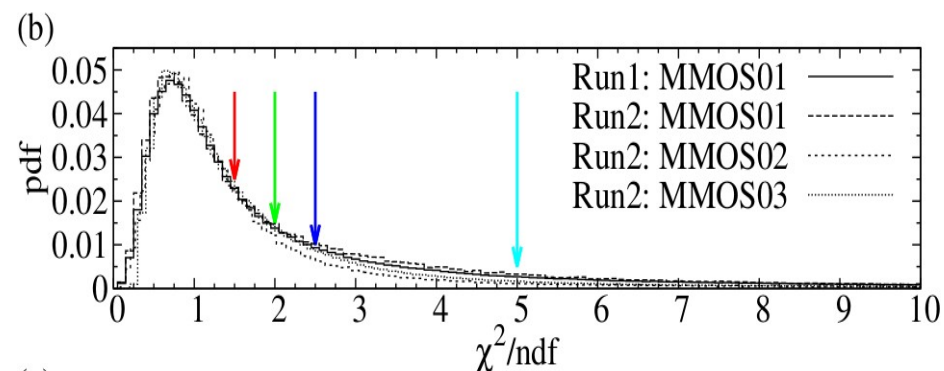
# Track Reconstruction and Analysis Methods

- Event-by-event offline track reconstruction (slopes in 1+1 dim and  $\chi^2/\text{n.d.f.}$ ) was applied independently for each MMOS module
- Pre-analysis was applied for alignment of detector layers and exclusion of noisy or malfunctioned electronics channels
- Track selection was based on  $\chi^2/\text{n.d.f.}$

See more at <https://doi.org/10.1038/s41598-018-21423-9>

- GEANT4-based detector simulations were applied to set energy cuts of muons to approx. 1 GeV that corresponded to  $\chi^2/\text{n.d.f.} < 1.5$
- Directions of different MMOS modules were oriented to the reference direction that was  $30.25^\circ$  from North and horizontal
- Muon fluxes were weighted with the inverse of their relative errors, and thereafter averaged

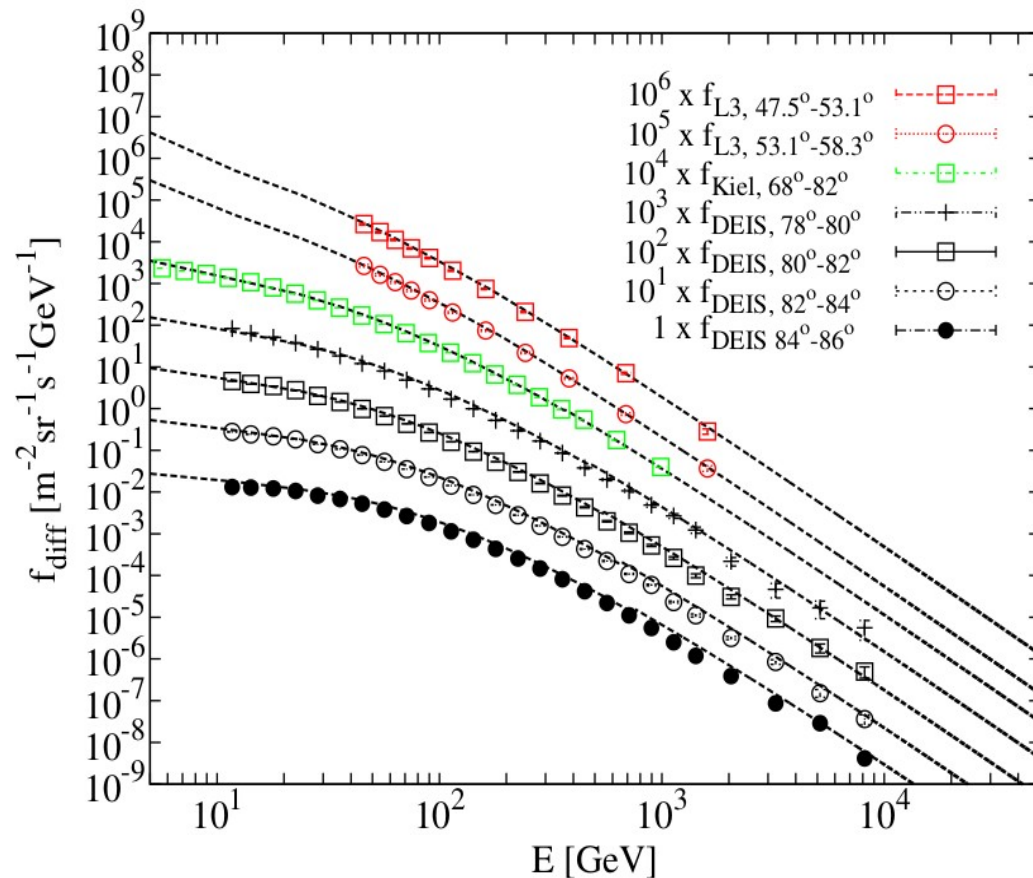
See more at <https://doi.org/10.1029/2019GL084784>



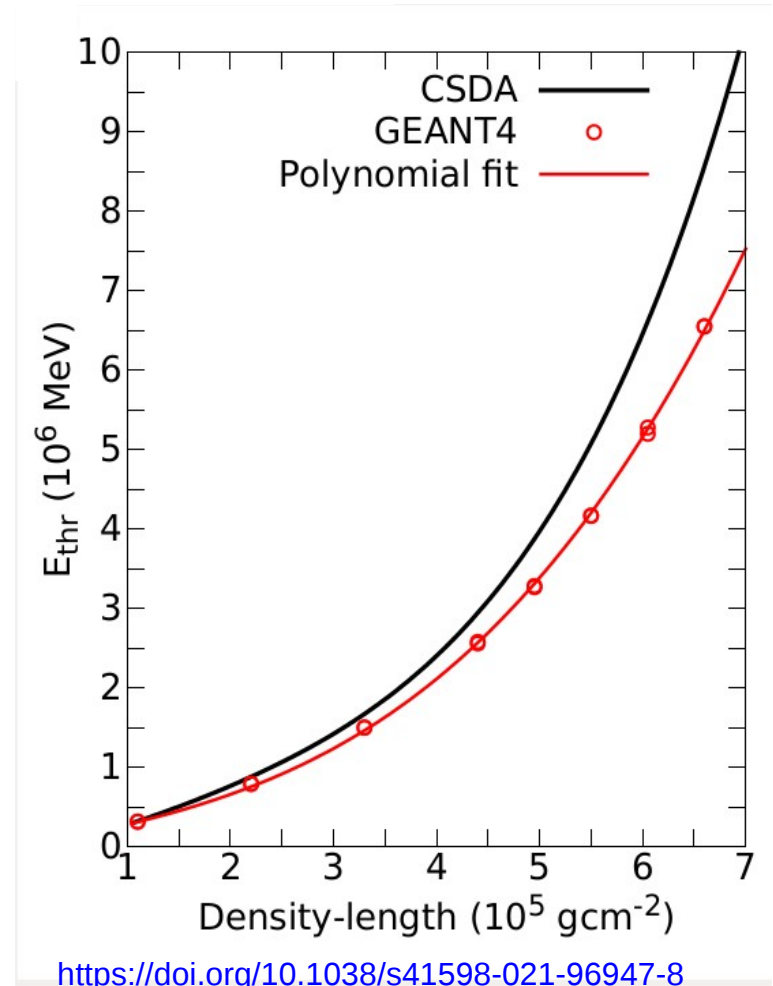
# Numerical and Simulation Methods

Density-length is determined by means of comparison of calculated fluxes to the measured values:

$$F_{calc}(90^\circ - \theta_y, L) = \int_{E_{thr}(L)}^{\infty} f_{diff}(E, 90^\circ - \theta_y) dE$$



<https://doi.org/10.1038/s41598-018-21423-9>



<https://doi.org/10.1038/s41598-021-96947-8>

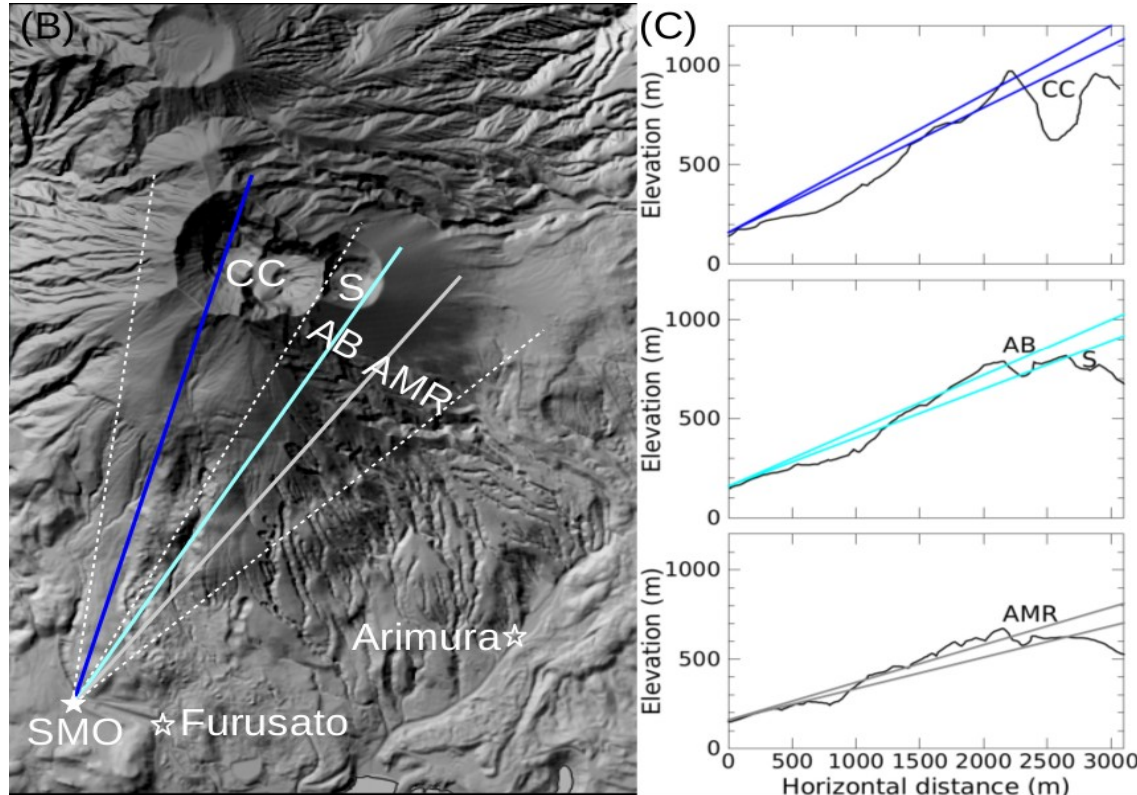
# III. Muographic Monitoring of Tephra Deposition and Erosion

# Indirect Volcanic Hazards



Lahars are fast-moving gravity-driven flows of mixture of volcanic rocks and water occurred either during eruptions or when the volcano is dormant.

Wind and water driven erosion processes can destabilize and mobilize the tephra deposition before they become fully incorporated into the soil.



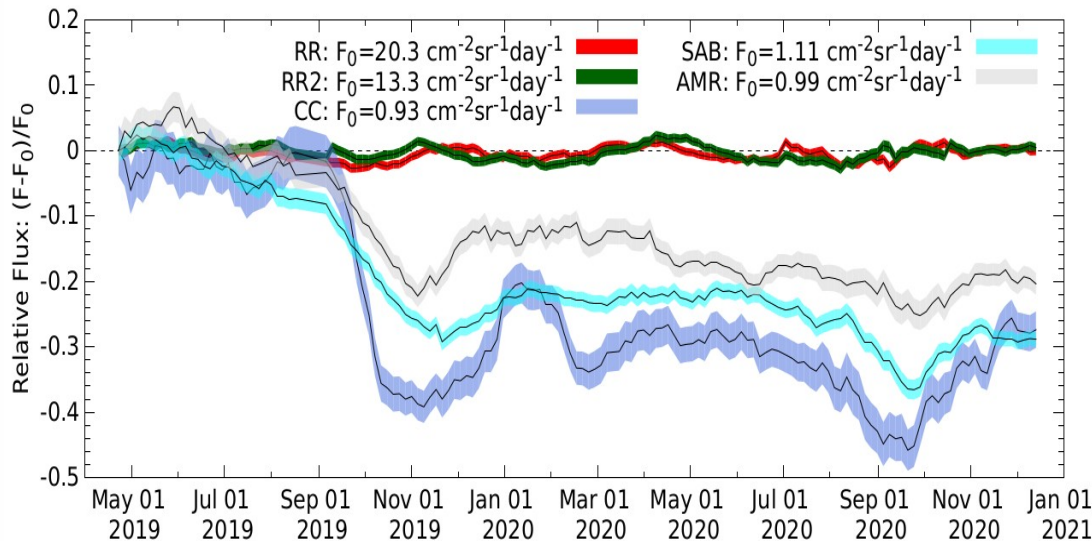
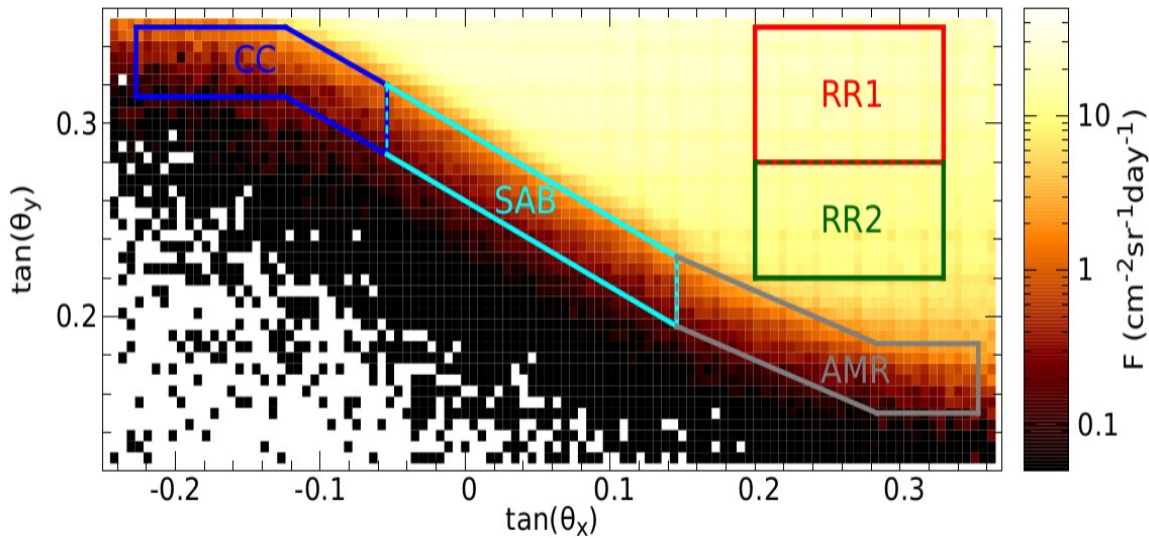
The generation and dynamics of lahars are controlled by the following factors:

- (i) local topography,
- (ii) volcanic activity,
- (iii) amount and composition of tephra,
- (iv) intensity and duration of rainfall.

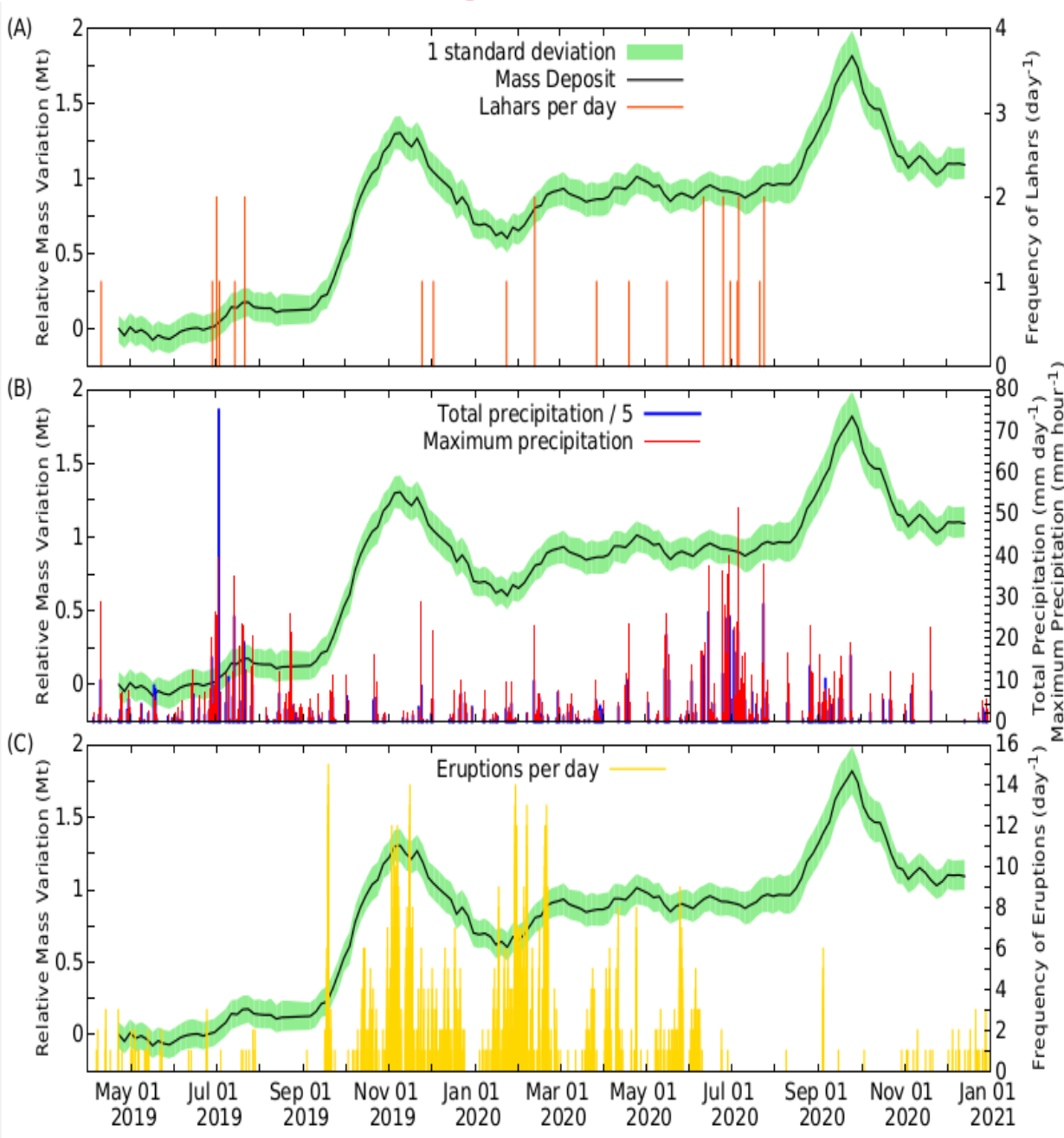
**Muography has potential to measure the amount (mass and thickness) of tephra deposition and topographical changes that controlling the onset of post-eruptive lahars.**

# Muographic Observation of Tephra Deposition

- Muon flux was monitored through the
  - Central Craters (CC),
  - Showa and Arimura Basin (SAB),
  - Arimura Middle Reaches (AMR),
  - two reference regions (RR1 and RR2).
- **The fluxes were averaged** in each angular region for time-intervals of 4 days, and the averaged fluxes were smoothed by applying a moving average calculated from the previous ten consecutive time-intervals, i.e. **over a period of 40 days**.
- **After September 2019, the relative averaged fluxes (measured relatively the flux of the first time sequence,  $F_0$ ) decreased through the volcano regions from 10 to 40%.**
- Change of volcanic ejecta mass that was measured to approx. 0.25 Mt between April and September 2019 and approx. 2 Mt from September 2019 to July 2020 by the Japan Meteorological Agency



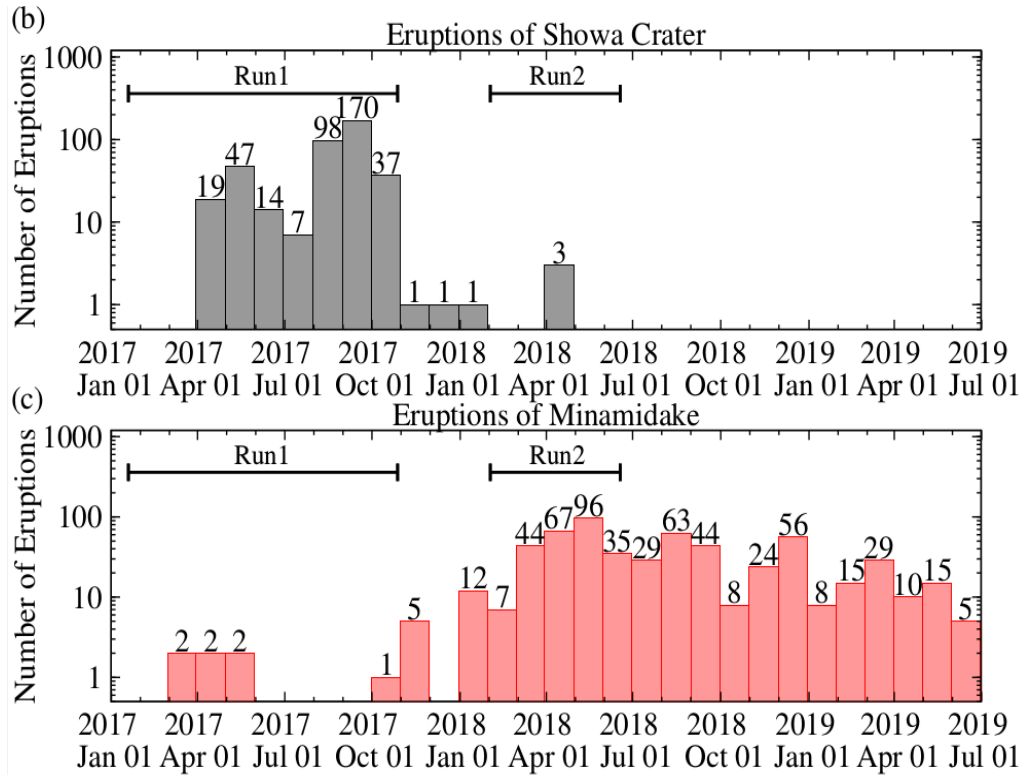
# Muographic Observation of Erosion



- The total mass (volcanic edifice and tephra) was measured to  $M_0 = (7.54 \pm 0.05)$  Mt during the 1st time-interval → **Relative mass variation ( $M - M_0$ )** was quantified
- **Mass deposit showed significantly decreasing trends** through various periods, e.g. from November 2019 to January 2020, during March 2020 and October 2020:
  - (i) The volcanic sediments were transported from the selected peak regions to downstream regions of the volcano **by the onset of rain-triggered lahar events.**
  - (ii) Further mass decreases were observed without the occurrence of lahar events, e.g. after mid-September 2020. This observation suggests the **water driven erosion of the peak region of Sakurajima volcano.**

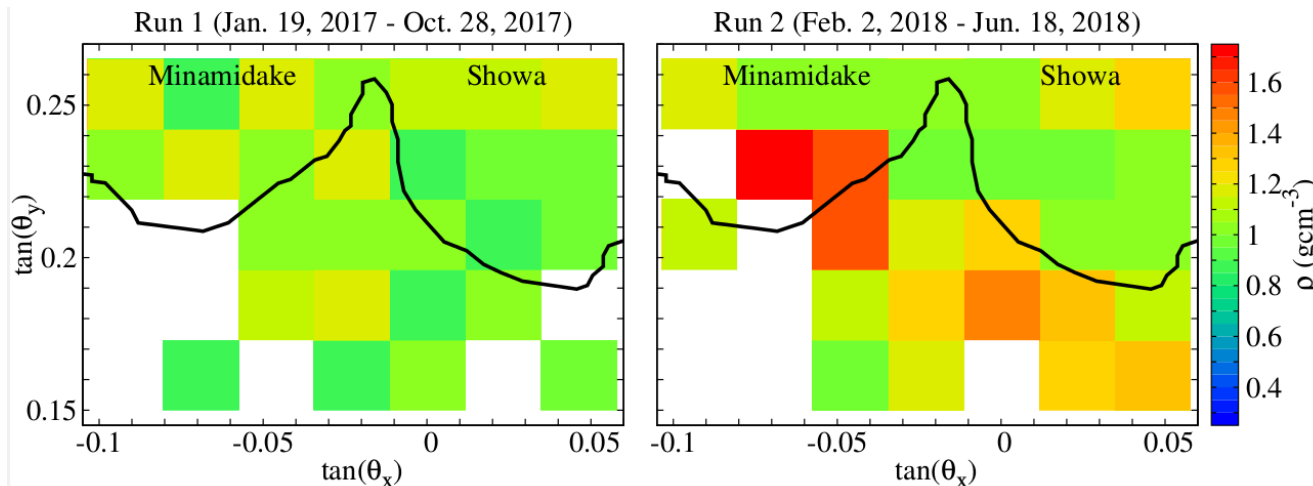
# IV. Muography of Magmatic Plug Formation

# Deactivation of Showa Crater



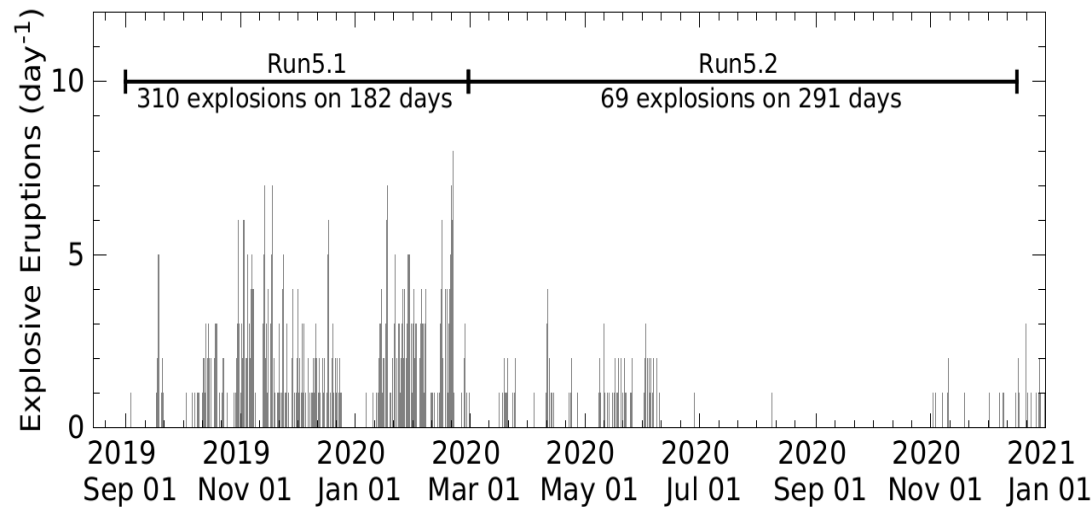
- **What is the cause of the shift of eruption sequence from Showa to Minamidake?**
- Two data sets were analysed:  
Run 1: January - November 2017;  
Run 2: February - June 2018.
- Systematics effects on muon flux: < 5 %

See more in <https://doi.org/10.1029/2019GL084784>

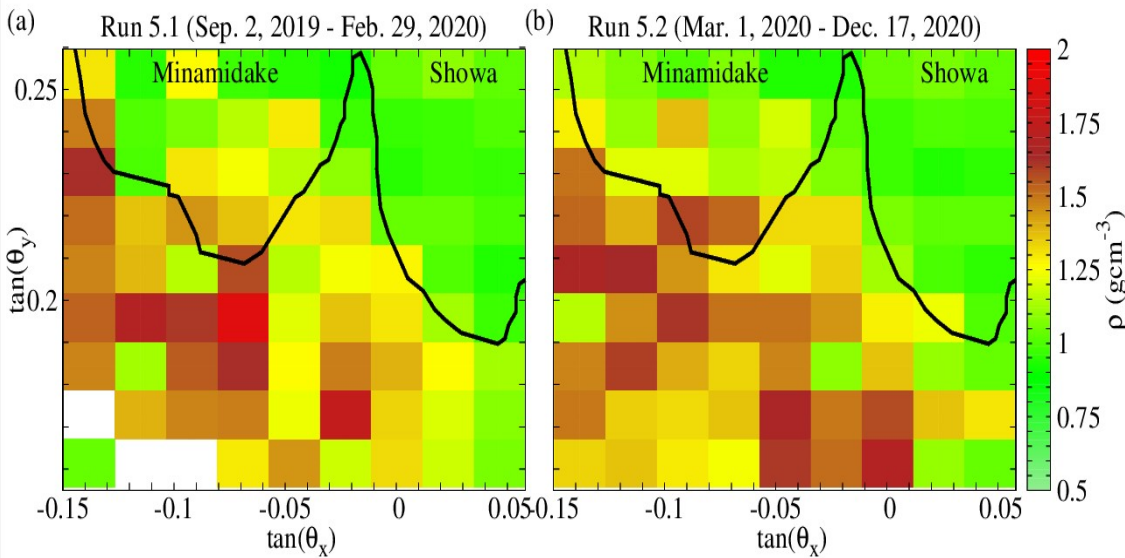


- Significant density increase from  $2\sigma$ - $4\sigma$  was observed bin-by-bin across Minamidake and beneath Showa crater ( $\sim 7$  Mt)

# Decreased Activity of Minamidake Crater



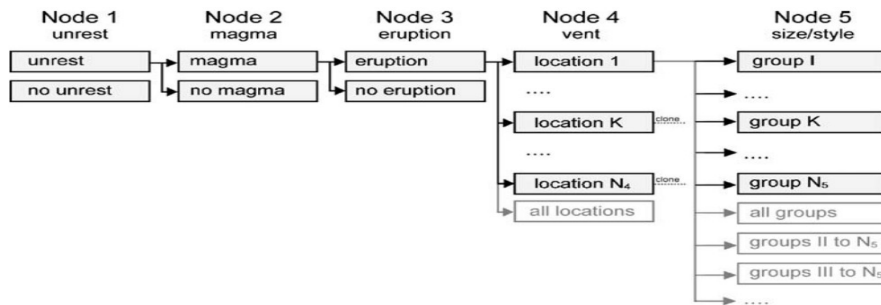
- We assume the existence of a low-density, debris-filled volume under the two craters that acts as a magma reservoir. The lateral extension of this volume is estimated to be approx. 300 m at depth of 100-200 m.
- Liquid magma fills the inter-grain spaces in this volume a few tens of minutes before the onset of eruption.
- After the eruption, the liquid magma is drained back to the conduit.
- Thereafter, the solidification of this volume creates a magmatic plug under the crater. The decreasing of the permeability of this volume explains the deactivation of the Showa crater in April 2018 and the latest dormant periods of Minamidake crater from March to December 2020.



# **V. Eruption Forecasting by Machine Learning of Muographic Data**

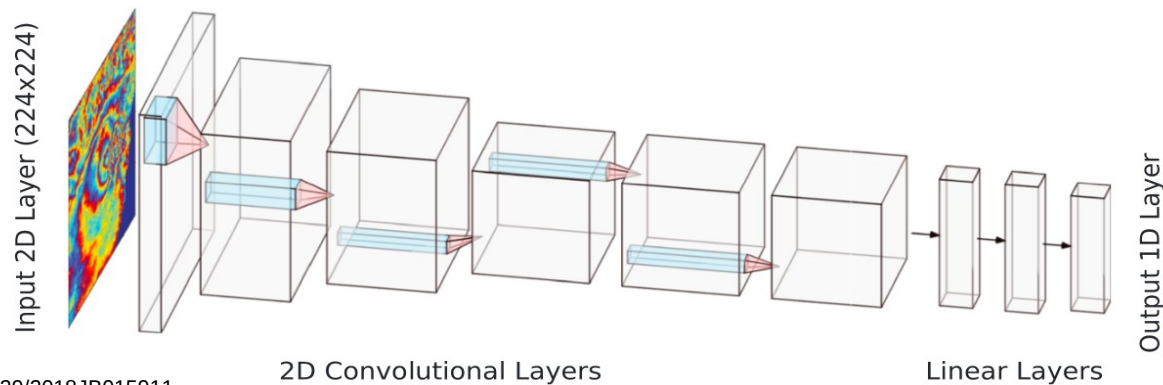
# Eruption Forecasting

- Bayesian Event Trees for **long-term eruption forecasting**



Source: <https://doi.org/10.1007/s00445-009-0311-9>

- Convolutional Neural Networks for classification of volcanic deformation and **short term eruption forecasting**

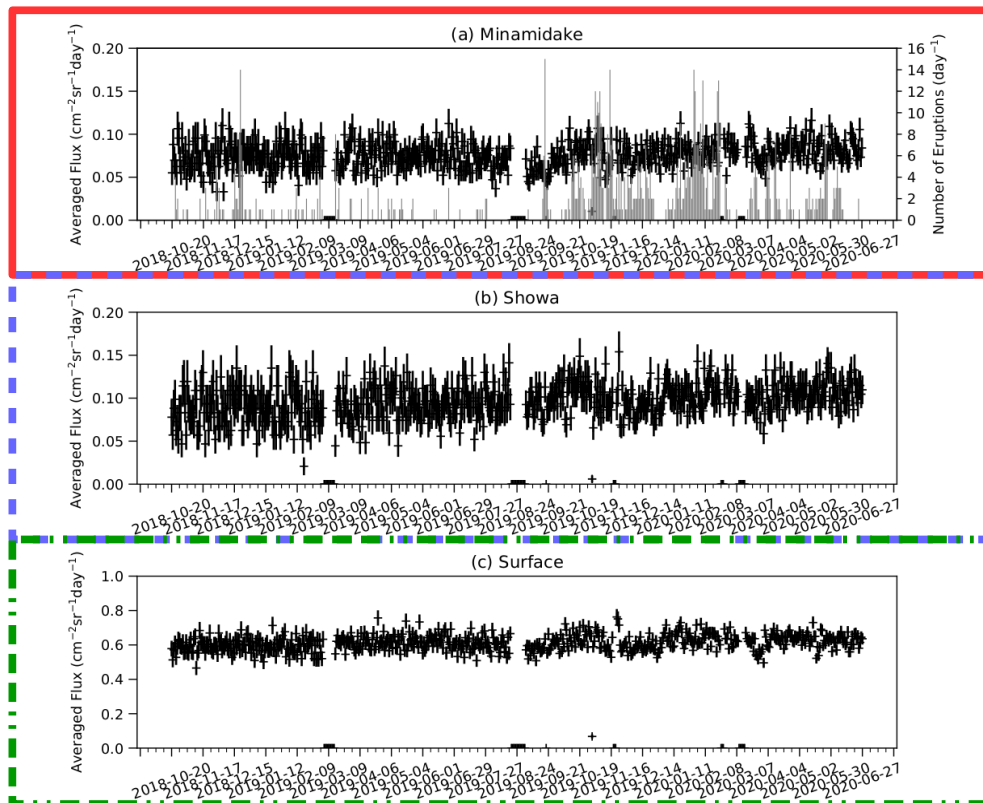


Source: <https://doi.org/10.1029/2018JB015911>

- Goal:** real-time eruption forecasting by machine learning of muographic data

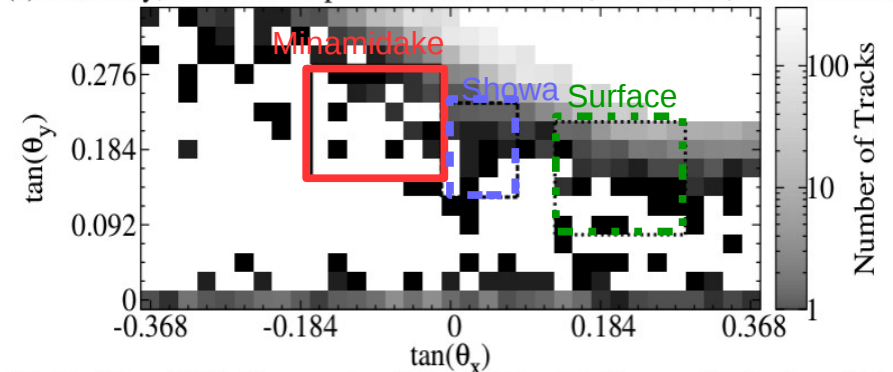
# Preparation of Data to Supervised Machine Learning

- Daily muograms were determined for period from October 2018 to June 2020
- **Average flux values and sub-images** were extracted from three selected regions:
  - Active **Minamidake** crater,
  - Dormant **Showa** crater,
  - **Surface** region.
- **Eruption labels** were also derived to all days  
**Eruption**  $\rightarrow$  1, **No eruption**  $\rightarrow$  0

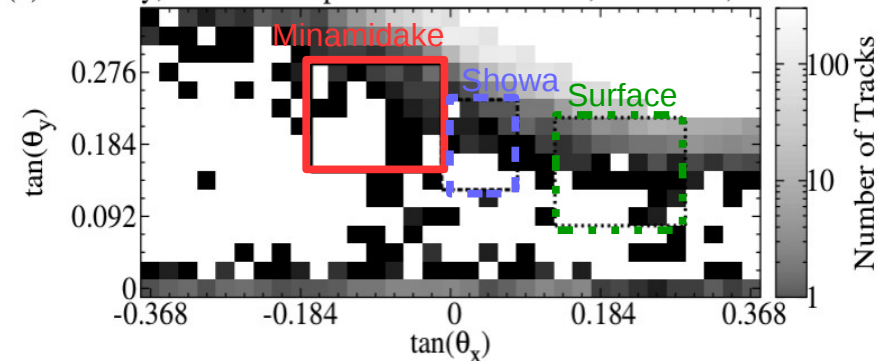


Muographic image resolution:  
 23 mrad x 23 mrad  $\rightarrow$  60 m x 60 m

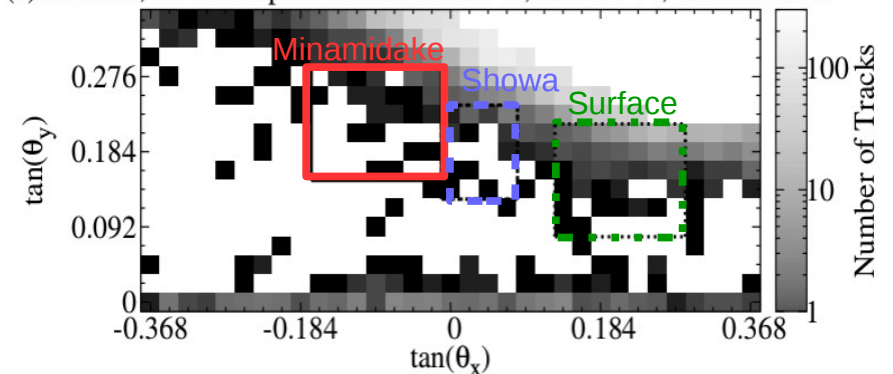
(a) 30th May, 2020: No eruption. Minamidake: 43, Showa: 53, Surface: 356.



(b) 31st May, 2020: No eruption. Minamidake: 56, Showa: 35, Surface: 316.

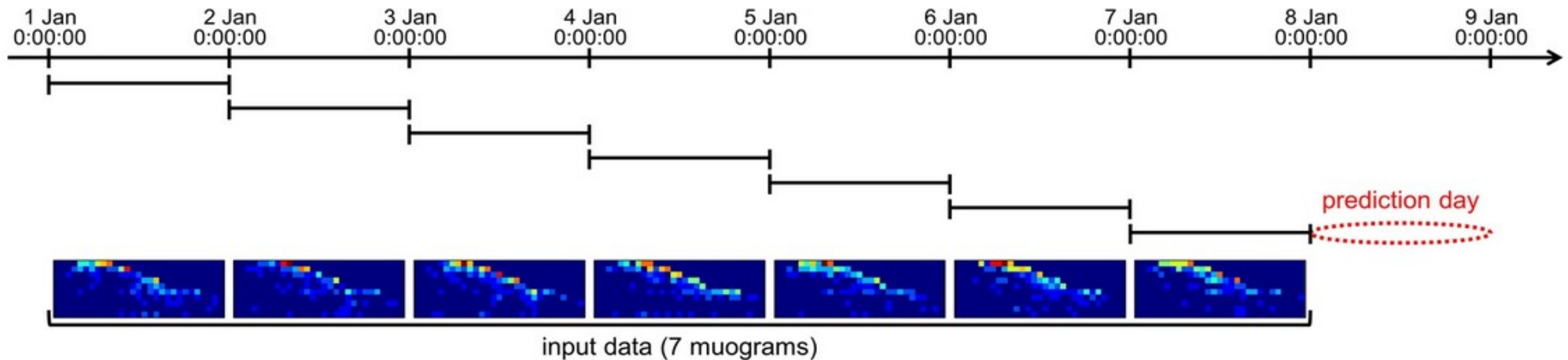


(c) 1st June, 2020: Erupted. Minamidake: 46, Showa: 44, Surface: 361.



# Cocept of the Study

This study applied the concept that was developed by Nomura et al. for forecasting of the eruptions of Showa crater and achieved a ROC AUC of 0.726 (<https://doi.org/10.1038/s41598-020-62342-y>) using the data collected with two scintillator-based tracking systems (<https://www.nature.com/articles/s41598-020-71902-1>) between 2014 and 2016.



The data collected by the MWPC-based tracking system for forecasting the eruptions of Minamidake crater were organized as follows.

**Training data:** 394 days with 146 eruption days (only Minamidake erupted)

**Validation data:** 110 days with 48 eruption days (only Minamidake erupted)

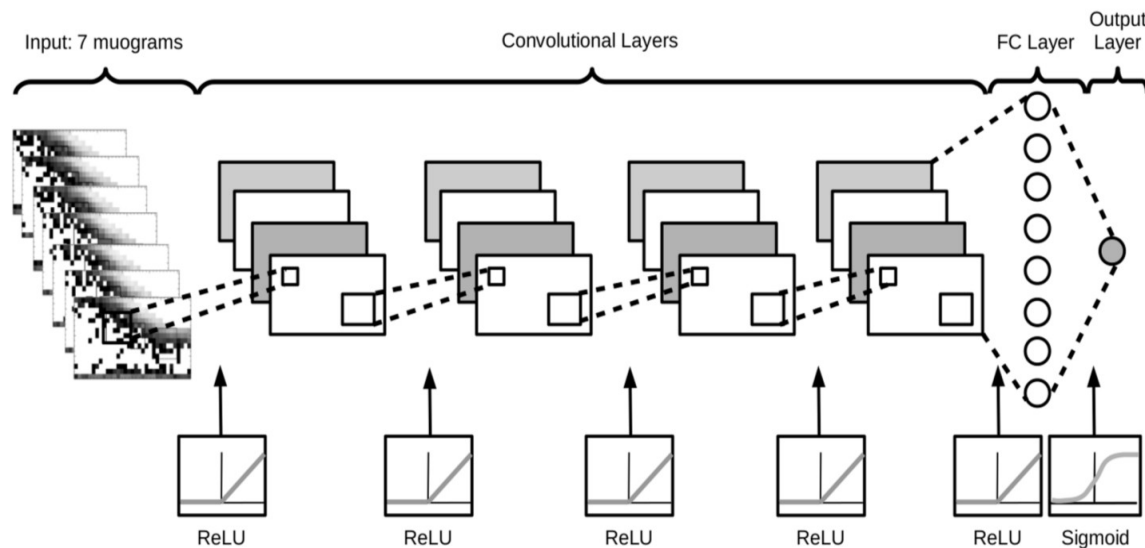
**Test data:** 109 days with 56 eruption days (only Minamidake erupted)

**Applied Software:** scikit-learn version 0.22.1, Keras version 2.4.3 and Tensorflow version 2.3.0

**Receiver Operating Characteristic (ROC) analysis** was applied to determine eruption forecasting performances

# Learning of Muographic Images with Convolutional Neural Network

- Application of a series of convolutional layers allows to reveal the hidden features of images on layer-by-layer basis, and fully-connected neurons can process the extracted features to predict the eruptions. A fix filter size of 3x3 was used in this analysis.
- CNN was trained using Adam method.
- The hyperparameters of the CNN model were tuned with Bayesian optimization and selected by ROC analysis. The Number of epochs was found to be 100 and number of early patience was found to be 10.

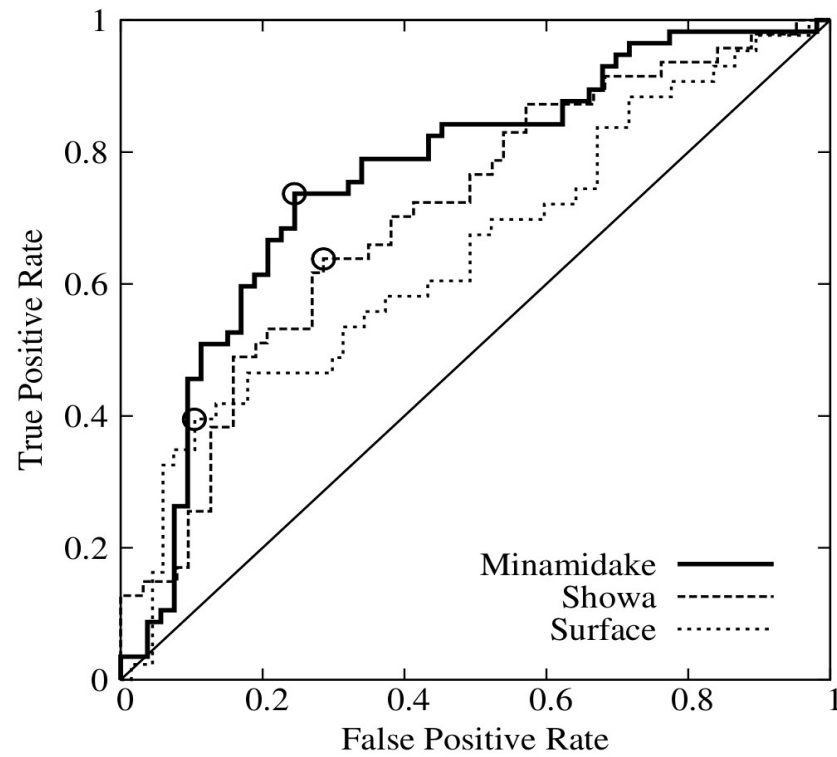
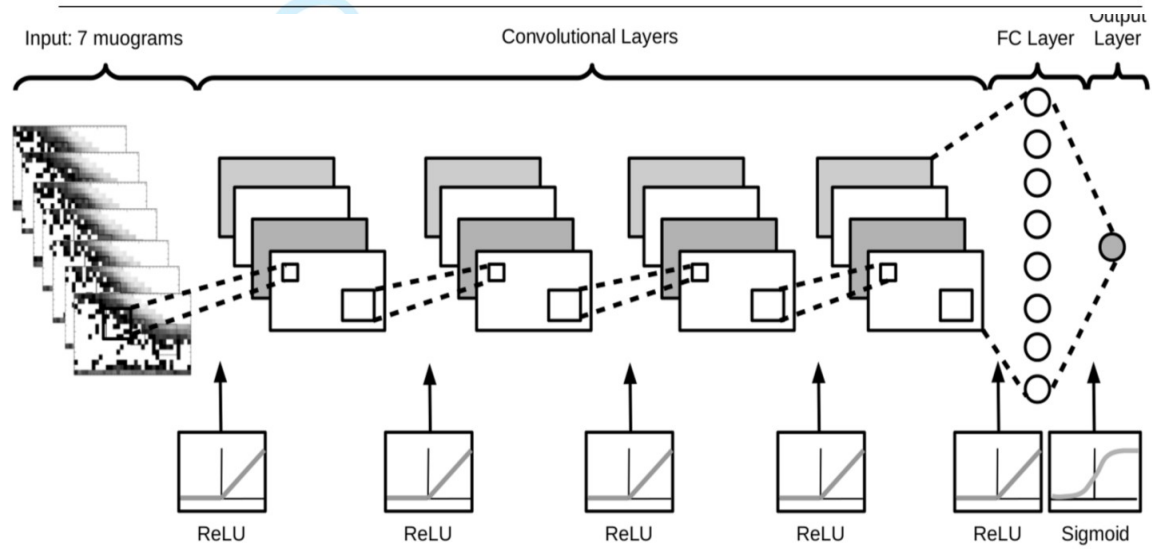


Region	Minamidake	Showa	Surface
Convolutional Layers	2	2	3
Filters on 1st Conv. Layer	16	64	8
Filters on 2nd Conv. Layer	64	32	8
Filters on 3rd Conv. Layer	-	-	4
Neurons on FC Layer	32	128	32
Dropout	0.215	0.313	0.332
Batch Size	16	8	32
Learning Rate	0.000448	0.002749	0.00002
Decay Rate	0.926	0.969	0.981

# Learning of Muographic Images with Convolutional Neural Network

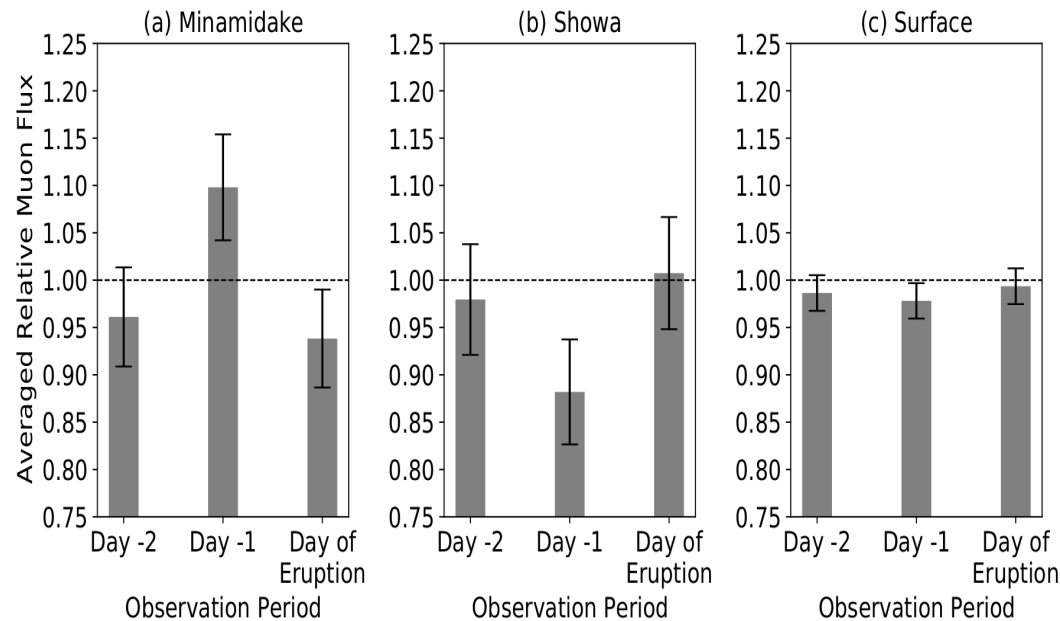
- Application of a series of convolutional layers allows to reveal the hidden features of images on layer-by-layer basis, and fully-connected neurons can process the extracted features to predict the eruptions. A fix filter size of 3x3 was used in this analysis.
- CNN was trained using Adam method.
- The hyperparameters of the CNN model were tuned with Bayesian optimization and selected by ROC analysis. The optimal number of epochs was found to be 100 and number of early patience was found to be 10.
- Results of ROC analysis showed that **CNN achieved a fair AUC of 0.761 in Minamidake from the eruptions occurred**

	Minamidake	Showa	Surface
Area Under the Curve	0.761	0.704	0.644
Sensitivity	0.737	0.638	0.395
Specificity	0.755	0.714	0.896



# Discussion and Future perspectives

- **Comparison to the results of Nomura et al. (forecasting of Showa's eruptions with ROC AUC of 0.726) and this work (forecasting of Mindamidake's eruptions with ROC AUC of 0.761):** Despite the application of upgraded muography observation system with enlarged (5 sqm  $\rightarrow$  8 sqm) sensitive surface area and higher angular resolution (33 mrad  $\rightarrow$  23 mrad), the forecasting performance was not drastically improved probably due to the following reasons:
  - smaller number of eruptions occurred in Minamidake (832) than in Showa (1432) that resulted in smaller amount of training data,
  - smaller amount of mass was transported beneath the Minamidake than Showa that resulted in smaller variations in muographic images,
  - the geometrical difference between the two craters is also assumed to be an influencing factor.



- **Future Perspectives:**

- The upgrade of the MMOS is planned to collect more data  $\rightarrow$  MAGMA
- Recurrent Neural Network with Long-Short Term Memory is expected to improve forecasting
- Integration of muographic data with other remote sensing data
- CNN works as a black box function  $\rightarrow$  Interpretable machine learning

# VI. Summary

- MWPC-based Muography Observation System (MMOS) of Sakurajima Muography Observatory (SMO) is being under development in international collaboration since 2017  
<https://doi.org/10.1038/s41598-018-21423-9>
- **Volcanological applications with the MMOS:**
  - Monitoring of tephra deposition and erosion of volcanic edifice  
<https://doi.org/10.1038/s41598-021-96947-8>
  - Muographic imaging of plug formation beneath deactivated craters  
<https://doi.org/10.1002/9781119722748.ch08>  
<https://doi.org/10.1029/2019GL084784>
  - Machine learning of muographic data for volcano eruption forecasting  
<https://doi.org/10.1002/9781119722748.ch04>

## Contributors of Sakurajima Muography Project:

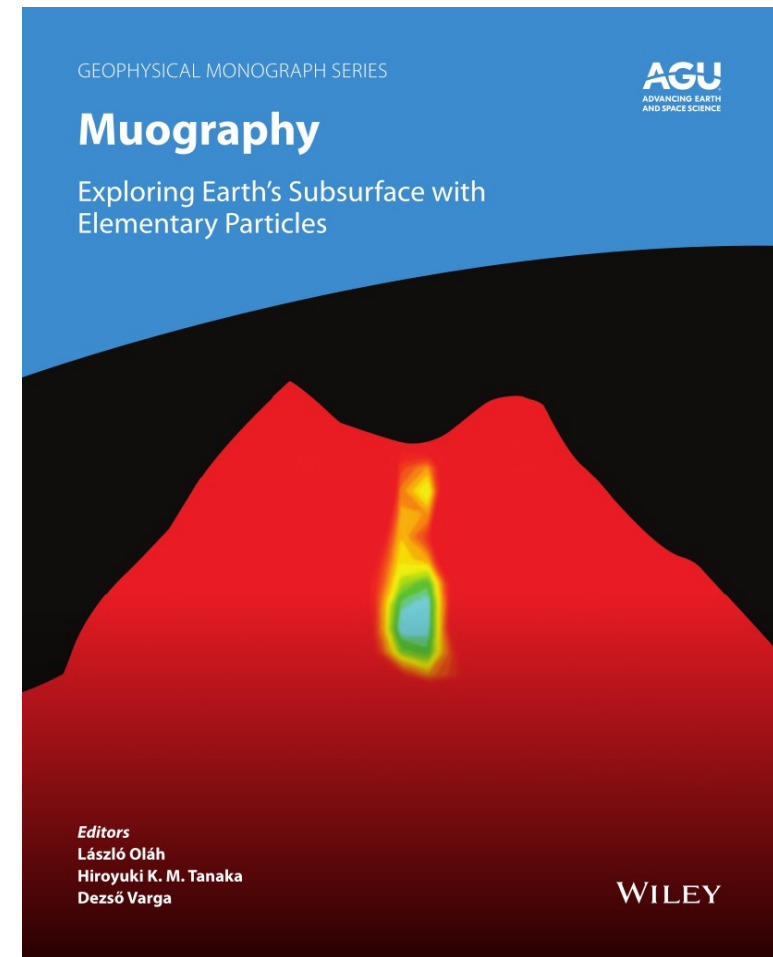
**The University of Tokyo:** L. Oláh, H. K. M. Tanaka, T. Ohminato

**Wigner RCP:** D. Varga, G. Hamar, G. Nyitrai, Sz. J. Balogh, Á. L. Gera, G. Galgóczi

Our work is supported by the Joint Usage Research Project (JURP) of the University of Tokyo, Earthquake Research Institute (ERI) under project ID 2020-H-05, the “INTENSE” H2020 MSCA RISE project under Grant Agreement No. 822185, the Hungarian NKFIH research grant under ID OTKA-FK-135349; Wigner Research Centre for Physics of the Eötvös Loránd Research Network and the Ministry of Education, Culture, Sports, Science and Technology, Japan (MEXT) Integrated Program for the Next Generation Volcano Research.

**Thank you  
for your attention!**

Oláh Muographers2021



## Contact information:

László Oláh

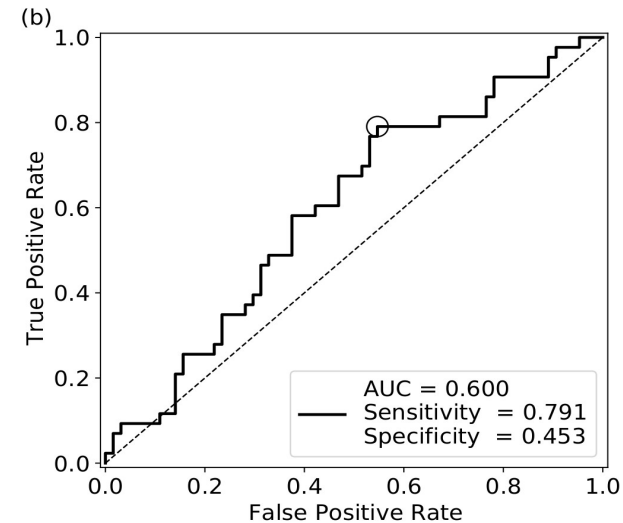
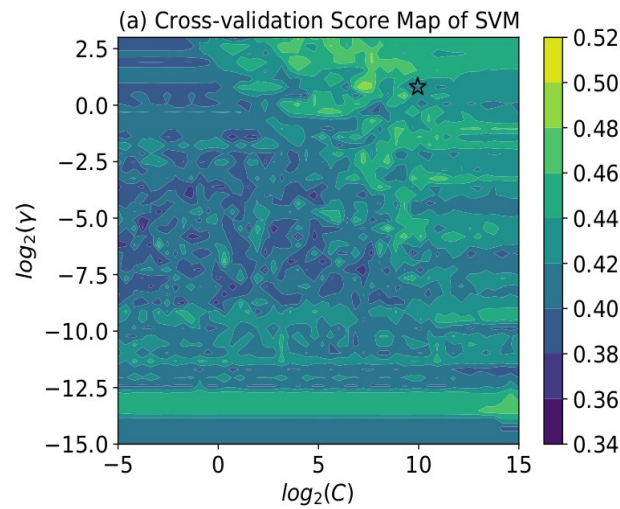
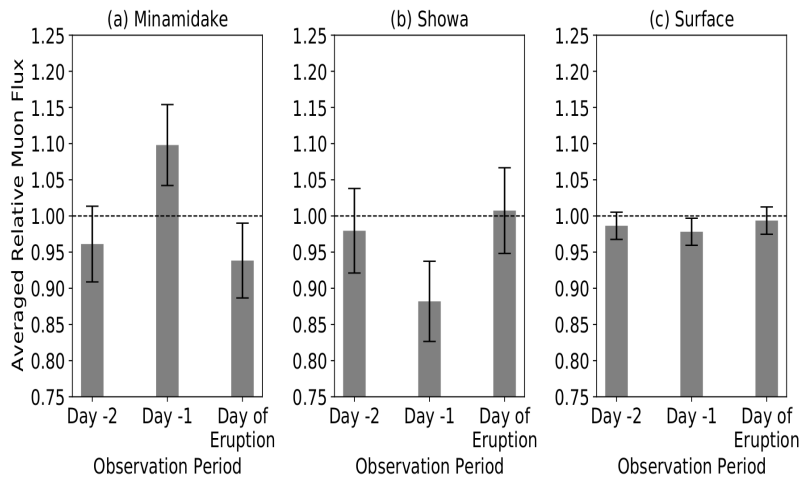
[olah.laszlo@wigner.hu](mailto:olah.laszlo@wigner.hu)

[olah@virtual-muography-institute.org](mailto:olah@virtual-muography-institute.org)

# Backup Slides

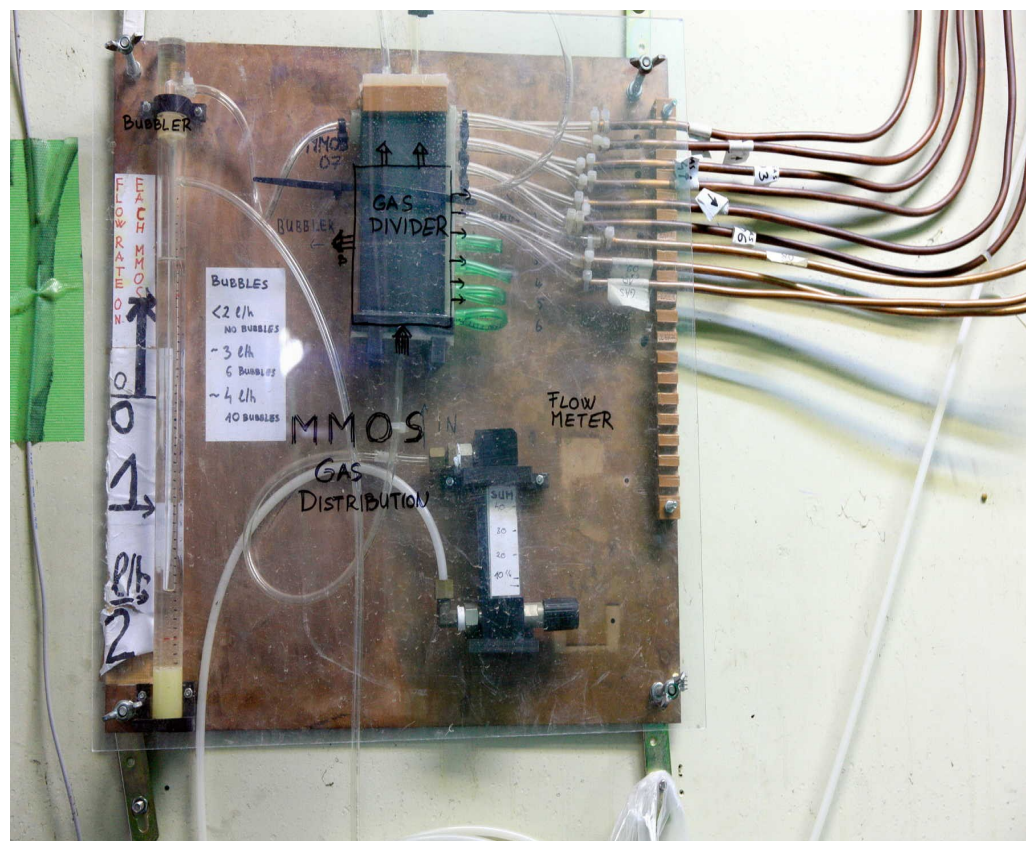
# Learning of Average Flux Values with Support Vector Machine

- Relative flux values were averaged for 16 turns: an increase above 2.5 sigma was observed 1 day before eruption hints the explosion of volcanic plug beneath Minamidake before eruption
- Support Vector machine with radial basis kernel (C and  $\gamma$  parameters) was trained with the average flux values and eruption labels from training data set
- Parameters were selected based on their cross-validation score:  $C=925.827$  and  $\gamma=1.74564$
- Results of Receiver Operating Characteristic (ROC) analysis using test data set:  
Moderate accuracy of 0.6  $\rightarrow$  SVM (and other ML models, e.g. ANN) can not capture the patterns created by uprision magma or plug explosion before the occurrence of volcano eruption



# Gas System of MMOS

- Detector operation is provided by continuous flow of non-flammable, non-toxic Ar-CO<sub>2</sub> gas mixture with a flow of 2 Liters/hour
- 3-5 months continuous operation by a cluster of gas bottles (a volume of 40 Liters at a pressure of 140 bars each)



# III. Automated Muographic Visualization Framework

